

Co-pyrolysis behaviors and kinetics of sewage sludge and pine sawdust blends under non-isothermal conditions

Xiaolei Zhu · Zhihua Chen · Bo Xiao ·
Zhiquan Hu · Mian Hu · Cuixia Liu ·
Qi Zhang

Received: 18 July 2014 / Accepted: 20 November 2014 / Published online: 24 December 2014
© Akadémiai Kiadó, Budapest, Hungary 2014

Abstract Mixing of sewage sludge with classical biomass, such as pine sawdust, can compensate the weaknesses of one fuel by another. The pyrolytic characteristics of sewage sludge (SS), pine sawdust (PS), and their blends were investigated under nitrogen atmosphere by dynamic thermogravimetric analysis at three heating rates of 10, 20, and 30 K min⁻¹. Three thermal stages (dehydration, devolatilization, further carbonization) were identified during the pyrolysis of single materials, as well as the blends. Blending of PS with SS can improve the devolatilization properties of SS, whereas the initial decomposition temperature increases with the increase in proportion of PS. It has been found that the pyrolytic characteristics of the blends can be estimated from those of parent fuels, suggesting that no significant synergistic effect existed during thermal degradation of PS/SS blends. The dependence of apparent activation energy on conversion obtained by Friedman method and distributed activation energy model (DAEM) revealed that the blends can be considered as multistage process. The results indicated that the DAEM can provide reasonable fits to the experimental data.

Keywords Co-pyrolysis · Sewage sludge · Synergy · Kinetics

Introduction

Sewage sludge is regarded as the residue generated from municipal wastewater treatment plants, which encompasses

a vast amount of substances and microorganisms in suspended, or dissolved state [1]. Given the development of population and rapid urbanization all over the world, the sewage sludge yield in the near future would remain to be progressively increased. The treatment of the increasing amount of sewage sludge, in an economically and environmentally acceptable manner, is a topical issue of great significance. Currently, there exist mainly four traditional and commercial methods of sewage sludge disposal: recycling as a fertilizer, landfilling, dumping into sea, and incineration. However, each of these methods has its own defects and they do not belong to waste-to-clean energy conversion either. Furthermore, the legislation coming into force in the near future will powerfully block most of these avenues of sewage sludge processing [2]. Hence, it is urgent and essential to find a feasible solution to more efficient disposal or utilization of sewage sludge.

Sustainable heat and power generation from biomass are at the center of scientific and industrial interest on account of the increasing awareness about the continuous shrinking reserve of fossil fuels and the higher sensibility toward environment preservation from pollutants generated by conventional energetic systems [3]. Unlike fossil fuel, the classical biomass feedstocks (such as wood, agricultural residues etc.) do not take millions of years to evolve. They are available locally and abundantly, and more attractively, they do not seem likely to be depleted with consumption owing to the renewability. These biomass sources use solar energy through the process known as photosynthesis metabolize atmospheric carbon dioxide, which counteracts the increase in atmospheric carbon dioxide that results from biomass fuel combustion. For this reason the biomass can be deemed as a “carbon neutral” fuel. From the above one can conclude these classical biomass sources are suitable for modern applications for energy sector, fuels,

X. Zhu · Z. Chen · B. Xiao · Z. Hu (✉) · M. Hu · C. Liu ·
Q. Zhang
School of Environmental Science and Engineering, Huazhong
University of Science and Technology, Wuhan 430074, China
e-mail: huzqhust@126.com

and chemistry, to name but a few. In this study, pine sawdust was selected as the classical biomass sample for its abundant source in China.

Thermal methods are indisputably a promising, convenient, and effective alternative to dispose sewage sludge which must (and will) prevail in the coming decades [2]. Thermochemical conversions will give rise to a complete oxidation of the organics and also the toxic organics within the high temperature. Heavy metals are usually immobilized in the inorganic matrix [4]. The main objective of thermal processing of sewage sludge is using the stored energy in sewage sludge, and in the meanwhile, minimizing environmental impacts for purpose of meeting the increasingly stringent standards. Normally, thermal methods of sewage sludge utilization are preceded by dehydration. The majority of energy released during thermal processes is consumed to reduce the amount of moisture. When mixed with pine sawdust in appropriate ratio, it can help dilute the high moisture content problem of sewage sludge to some degree. Moreover, the blends of pine sawdust and sludge are suitable for continuous feeding, due to the lack of knowledge and studies regarding methods of feeding reactors with raw materials in pasty form. In addition, a significant advantage of pine sawdust with respect to coal and sewage sludge is that the contents of nitrogen and especially sulfur are low. Lower concentrations of both NH_3 and H_2S were obtained when cogasifying sewage sludge with straw pellets [5]. However, pine sawdust has a lower density compared to sludge that will be inclined to fly and float, their co-processing can compensate the weaknesses of one fuel by another; hence, boosting the efficacy of the overall process system.

The pyrolysis kinetics of solid fuels can obtain better, more informative results from the experiment, which can take to apply in theory and practice [6]. It is recommended that the methods using multiple heating rate programs can improve the accuracy of kinetic parameters [7]. Unfortunately, there are still a number of co-pyrolysis studies using only a single heating program to compute kinetic parameters, which on the contrary, produce unreliable or sometimes even nonsensical results. Therefore, it is reasonable to avoid using a single heating rate method. At present, there is no doubt that isoconversional methods are the quickest way to derive kinetic parameters for complex reaction profiles involving multiple processes [8]. Because of its applicability to a wide variety of temperature programs, the differential isoconversional method of Friedman is the most universal one among computationally simple methods. Moreover, it makes no mathematical approximations, thus producing no noticeable systematic error in the activation energy for the linear integral isoconversional method derived. However, this method is used rather rarely in actual kinetic analyses [9]. In addition, the distributed

activation energy model (DAEM) is considered as the best way [10] and has been widely used to represent mathematically the physical and chemical inhomogeneity of biomass and various ranks of coals [11–14].

Pyrolysis or devolatilization is not only a single process, but also the starting point for all other thermochemical conversion processes including combustion, gasification, and liquefaction, its sound understanding is of paramount importance for the effective use of pine sawdust, sewage sludge, and their blends. The main objective of this paper is to investigate the pyrolytic behavior of the blends of sewage sludge and lignocellulosic biomass, aiming to understand the impact of co-feed of biomass on sludge gasification and pyrolysis. Whether any interaction exists between sewage sludge and pine sawdust biomass in the solid phase or not during the pyrolysis process was also evaluated. The Friedman method and DAEM were applied to obtain the kinetics of both the individual materials and the blends. To validate the model, the fit between the experimental and simulated data was checked and presented.

Experimental

Samples

The sewage sludge produced in an urban wastewater treatment plant fed with municipal water was dewatered by filter press and then collected as one of the original materials in pyrolysis experiments. Another raw material (pine sawdust) was supplied by a farm in Wuhan City, Hubei Province, China. The samples were first dried at 378 K for 24 h in a drying oven to remove moisture prior to characterization, then both of them were ground and sieved by passing through a 120-mesh screen. The PS/SS blends were homogenized by mixing in several proportions (PS/SS 25:75, 50:50, and 75:25 mass%) and subsequent tumbling for 24 h. The proximate and ultimate analyses of the used pine sawdust and sewage sludge are shown in Table 1, together with the ash analysis.

Thermogravimetric analysis

Thermogravimetric analysis was performed up to 1,273 K at three heating rates (10, 20, and 30 K min^{-1}) with the solid samples using TG/DTA manufactured by PerkinElmer. A mass of approximately 10 mg was used in each case. To maintain the reacting atmosphere inert and limit the extent of the secondary reactions inside the particle, a 80 mL min^{-1} purge flow rate of nitrogen was introduced into the reactor. Under these conditions, one could eliminate mass and heat transfer limitations as well as the effects

of eventual side reactions to a great extent during the thermal decomposition.

Kinetics analysis

Friedman method

The conversion, α , can be calculated according to the following equation in pyrolysis reaction:

$$\alpha = \frac{m_i - m}{m_i - m_f}, \tag{1}$$

where m_i , m , m_f are the initial, actual, final masses of the sample, respectively.

The rate of a solid reaction, $d\alpha/dt$, can be formulated as

$$\frac{d\alpha}{dt} = k(T)f(\alpha), \tag{2}$$

where t and $k(T)$ are the time and the rate constant, respectively, and $f(\alpha)$ is considered the reaction model reflecting the mechanism of the process.

The temperature dependence of the rate constant k is generally parameterized through the Arrhenius equation

$$k(T) = Ae^{-\frac{E_A}{RT}}, \tag{3}$$

where T is absolute temperature (K), A is the pre-exponential factor (min^{-1}), E_A is apparent activation energy (KJ mol^{-1}), and R is the universal gas constant ($8.314 \text{ KJ mol}^{-1}$).

For experiments carried out at a linear heating rate $\beta = dT/dt$, combination of Eqs. (2) and (3) becomes

$$\frac{d\alpha}{dT} = \frac{A}{\beta} \exp\left(-\frac{E_A}{RT}\right) f(\alpha) \tag{4}$$

Taking natural logarithms of both sides from Eq. (4) gives

$$\ln\left(\beta \frac{d\alpha}{dT}\right)_{\alpha,i} = \ln[A_\alpha f(\alpha)] - \frac{E_A}{RT_{\alpha,i}}, \tag{5}$$

where the subscript i identifies an individual heating rate. Hence, at each given α , the activation energy E_A can be obtained from the slope of the plot of $\ln\left(\beta \frac{d\alpha}{dT}\right)_{\alpha,i}$ against $1/T_{\alpha,i}$.

Distributed activation energy model (DAEM)

The distributed activation energy model (DAEM) describes a complex reaction as an infinite number of irreversible first-order parallel reactions, each with its own activation energy and frequency factor. In the available literatures, there are some different methods solving the DAEM to establish the kinetic parameters. Please et al. [15] used asymptotic method to make exact approximations to the integrals to rapidly arrive

Table 1 Characteristics of PS and SS

Sample	Sewage sludge	Pine sawdust
Ultimate analysis (dry basis, %)		
C	18.09	48.21
H	3.23	6.54
N	3.02	0.77
S	0.23	0.09
O ^a	16.81	42.88
Proximate analysis (dry basis, %)		
Ash	58.62	1.51
Volatile	37.97	79.71
Fixed carbon	3.41	18.78
High heating value (MJ kg ⁻¹ , dry basis)	14.79	17.80
Ash analysis (mass%)		
Al ₂ O ₃	18.10	4.00
SiO ₂	46.17	9.83
P ₂ O ₅	9.73	1.71
SO ₃	2.06	1.68
K ₂ O	4.58	2.64
CaO	5.04	50.75
TiO ₂	1.26	0.66
MnO	0.57	0.20
Fe ₂ O ₃	12.09	28.53
CuO	0.13	–
ZnO	0.18	–

^a By difference

at the solution, thus reducing computation time. Cai and Ji [16] used a pattern search method to determine DAEM kinetic parameters. In this study, the kinetic analysis is performed based on the Miura–Maki integral method of the distributed activation energy model [17]. This integral method requires only three different heating rates without no prior assumptions for the formation of the activation energy distribution, proposed by the following Arrhenius-type equation:

$$\ln\left(\frac{\beta}{T^2}\right) = \ln\left(\frac{kR}{E}\right) + 0.6075 - \frac{E}{RT} \tag{6}$$

Accordingly, the slope of the curve $\ln\left(\frac{\beta}{T^2}\right)$ versus $1/T$ yields the activation energy. To check and present the fit between the model and the experimental data, a simplified procedure is used as described by Soria-Verdugo et al. [18].

Results and discussion

Pyrolysis characteristics of single materials

Figure 1 presents the results of TG analysis at the heating rate of 10 K min^{-1} , which show the mass loss and the rate

of mass loss for pine sawdust and sewage sludge single materials between 373 and 1,273 K; that is, after the evaporation of any free moisture. It is noticeable that the thermal degradation of both PS and SS can be divided into two main stages in general. As can be clearly seen, the temperature interval in which PS experiences the major mass loss is from 423 to 823 K, while the second pyrolysis stage continues at a much slower rate till the experiment completion. According to Yang et al. [19], hemicellulose is degraded easily first in the temperature range 493–588 K, and the pyrolysis of cellulose follows at 588–673 K, with that of lignin continuing from 423 to 1,173 K. Hence, for PS, it seems likely that the lower temperature shoulder located on the left represents the degradation of the thermally unstable hemicellulose, then the following outstanding point at higher temperatures in the right hand side is attributed to the decomposition of cellulose. In contrast with cellulose and hemicellulose, the decomposition of lignin covers over a very wide temperature range, providing thus a gently sloping baseline of the DTG curve.

Nonetheless, in the last pyrolysis step, a sharp peak completely isolated appears at temperature higher than 923 K, which is rarely reported by similar sample. Such temperature is typical of the dissociation of strongly bonded carbonate salts in these conditions. Whitely et al. [20] took advantage of some species-specific techniques (such as FTIR-MS) in consort with thermogravimetry analysis to facilitate the analysis of product gas under the same pyrolysis conditions, proving that an intense carbon dioxide evolution is noted in correspondence with the last peak of degradation. Therefore, it can be assumed that this peak is closely related with the thermal decomposition of metal carbonates. As reported in Table 1, the results using XRF on mineral analysis present that calcium contained in samples accounts for more than half of mineral matter content. According to these analyses, it can be deduced that

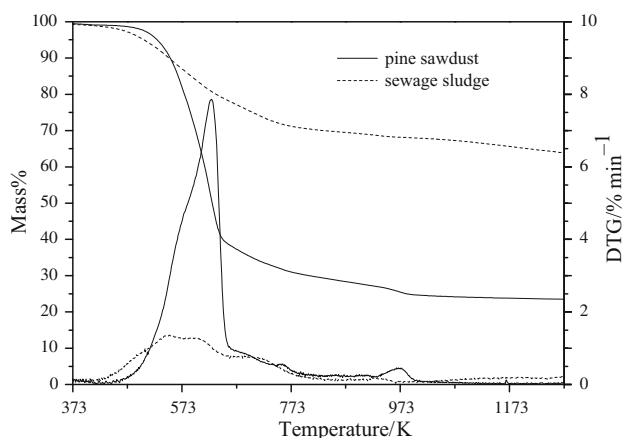


Fig. 1 TG and DTG curves of individual materials pyrolysis at 10 K min^{-1}

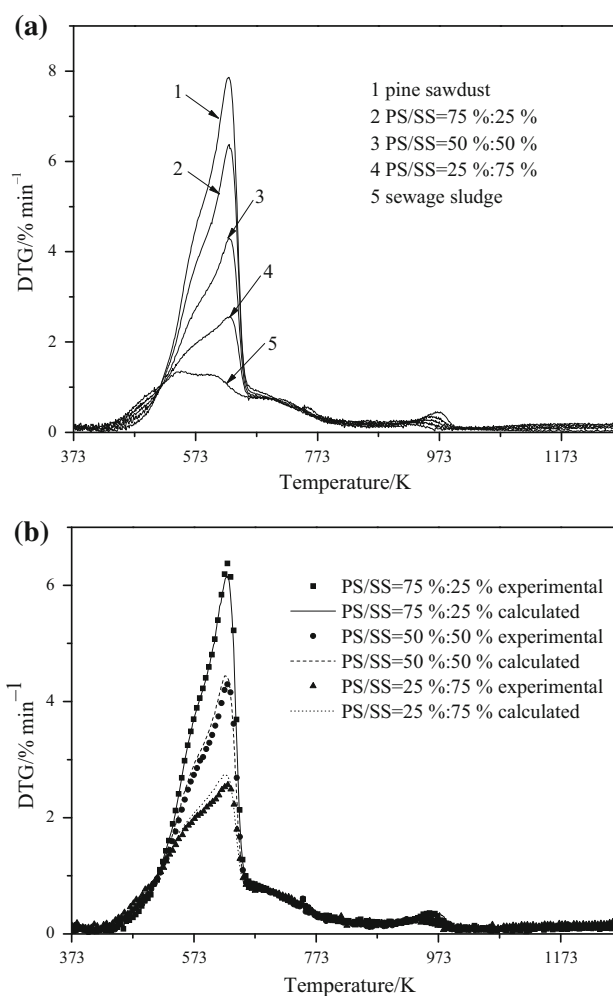


Fig. 2 **a** DTG curves for co-pyrolysis of PS and SS, **b** the comparison of experimental and calculated DTG curves for all blends at 10 K min^{-1}

the third peak is caused by the decarbonation of calcium carbonate under pyrolytic condition. Moreover, the TG analysis of calcium carbonate gave a further confirmation of this supposition in the same conditions [21].

In the case of SS, it had a lower thermal ability starting at approximately 403 K, and followed by a major loss of mass which is essentially completed up to 823 K at a relatively low and constant rate. The second pyrolysis stage continued a modest mass loss till the test completion, involving primarily the mineral matrix. In the first stage, the DTG curves exhibits two intense overlapping peaks and one pronounced shoulder with successively lower maximum reaction rates. Therefore, it presents two different types of organic volatiles being generated. The first two peaks may be concerned with the decomposition of thermolabile components of the organic matter such as proteins and carboxyl groups at approximately 573 K. At higher temperature ($\sim 723 \text{ K}$), the pronounced shoulder may be

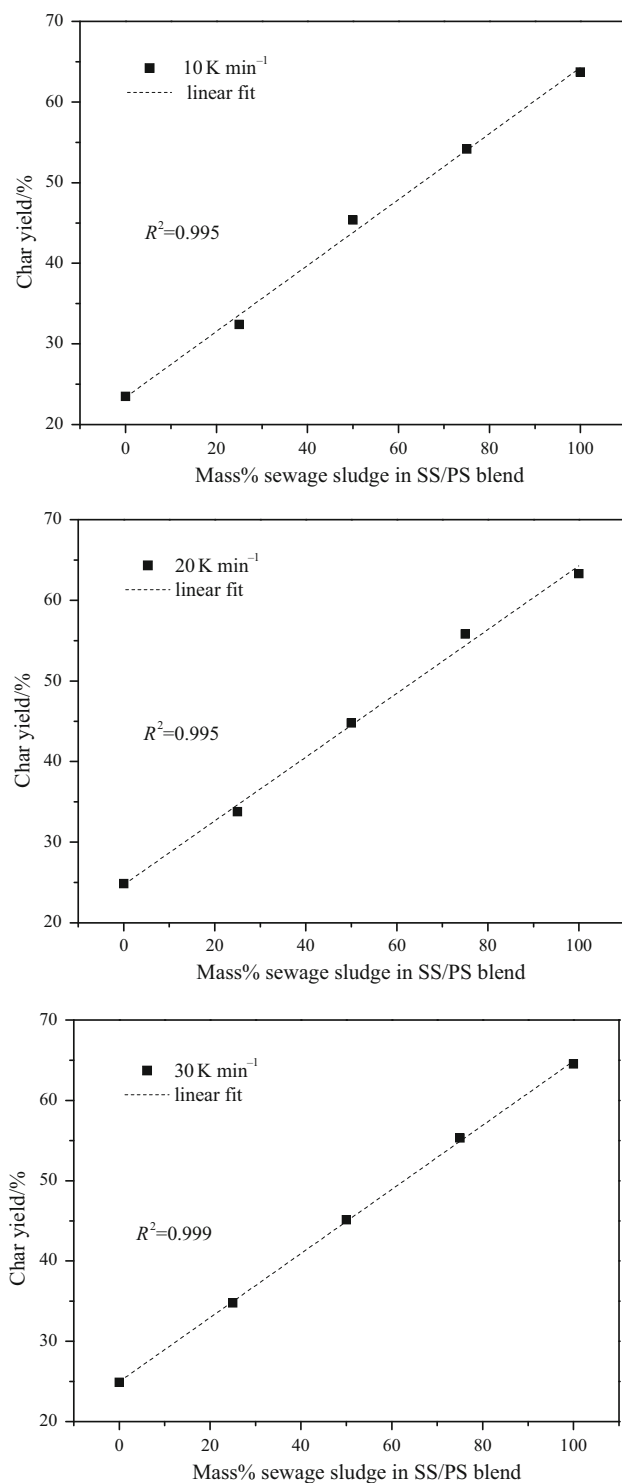


Fig. 3 Influence of SS/PS ratio on char yield at three different heating rates

caused by the decomposition of carbon refractories corresponding to a smaller fraction, such as the cracking aromatic ring, long-chain *N*-alkyl structures, and some saturated aliphatic chains [22]. However, the second stage

Table 2 Characteristic parameters at different heating rates

Sample	Heating rate/K min ⁻¹	T_{\max}^a /K	D_{\max}^b /% min ⁻¹	M_R^c /%
Pine sawdust	10	627.62	7.86	23.47
	20	640.86	15.40	24.87
	30	650.01	22.20	24.89
PS/SS = 75:25 %	10	628.15	6.38	32.39
	20	643.12	12.19	33.79
	30	652.23	20.42	34.79
PS/SS = 50:50 %	10	628.11	4.30	45.36
	20	643.11	8.90	44.79
	30	654.20	12.71	45.12
PS/SS = 25:75 %	10	628.80	2.56	54.16
	20	642.32	4.91	55.81
	30	652.09	7.41	55.30
Sewage sludge	10	549.80	1.36	63.70
	20	559.59	2.73	63.30
	30	571.33	4.10	64.53

^a Temperature of the maximum reaction rate

^b The maximum reaction rate

^c Pyrolysis residue mass

of SS pyrolysis is characterized by one small band centered at 973 K, mainly due to the decomposition of inorganic materials.

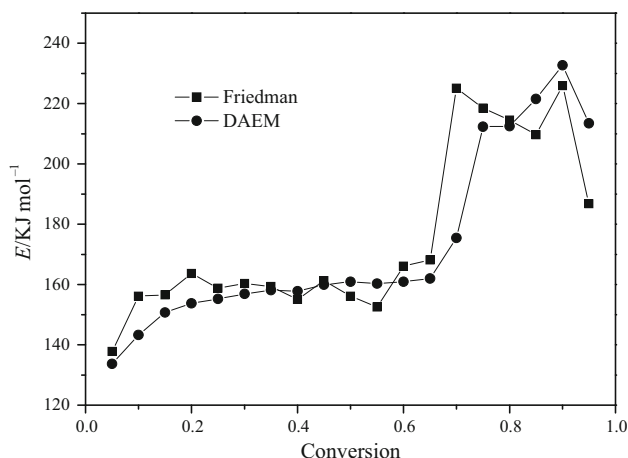
The temperatures at which the maximum mass loss occurs are 627.62 and 549.80 K, at a level of 7.86 and 1.36 % min⁻¹ for PS and SS, respectively. The reactivity can be evaluated from the DTG peak height and the temperature corresponding to peak height [23]. However, it seems difficult to draw conclusions regarding sewage sludge reactivity during pyrolysis, due to the uncertainty of measurement of other second peaks or shoulders presented in the DTG curves of SS. In addition, the total amount of volatiles from SS pyrolysis is approaching 26.30 mass% of its original mass, on a dry basis, while more than 76.53 mass% of the volatile matter is evolved for PS. This is in line with the proximate analysis results.

Pyrolysis characteristics of blends

The DTG profiles for the thermal degradation of the PS/SS blends compared with the pure samples, which were performed at the heating rate of 10 K min⁻¹, are illustrated in Fig. 2a. It can be seen clearly that the DTG curves of the blends were in between the ones of the parent materials. For all studied blends, the peaks representing sewage sludge and pine sawdust fractions of the blended materials maintained essentially the same shape within the same temperature range as when individual samples were pyrolyzed. Furthermore, the temperature at which the maximum

Table 3 Comparisons of the average value of apparent activation energy for all samples calculated by Friedman method and DAEM

Average E_A /KJ mol ⁻¹	Pine sawdust	PS/SS = 75:25 %	PS/SS = 50:50 %	PS/SS = 25:75 %	Sewage sludge
Friedman	155.56	154.96	152.39	175.39	151.39
DAEM	153.61	151.48	148.05	172.72	147.98

**Fig. 4** The relationship between the average E_A and various conversion rates determined by Friedman method and DAEM

conversion rate occurs in the blends in the DTG curves remained relatively unaltered when analyzed alone and in mixtures. However, the height of the shoulder and two peaks increased gradually as the percentage of biomass in the mixture increased, which signified a substantial enhancement of the volatile quantities released during thermal degradation.

By reason that synergy during most thermochemical processes cannot be isolated from the pyrolysis, one can narrow down where and why synergistic effect either exists or not in the co-conversion of SS and PS in thermochemical systems. In attempt to investigate whether synergistic effect existed in the case of co-pyrolysis between pine sawdust and sewage sludge at conditions typical of TG analysis (well-controlled slow heating rate), calculated curves based on a weighted sum of both reference materials' pyrolysis mass loss rate curves were obtained under the same conditions, according to Eq. (7). It can be concluded that there are no mutual interactions between the two individual materials, if the pyrolytic characteristics of the co-components follow the behaviors of the parent materials in an additive manner.

$$DTG_{\text{Blend}} = DTG_{\text{PS}}x_{\text{PS}} + DTG_{\text{SS}}x_{\text{SS}}, \quad (7)$$

where x_{PS} and x_{SS} are the proportions of pine sawdust and sewage sludge shares in the mixture, respectively; and DTG_{PS} and DTG_{SS} represent the mass loss rates of pine sawdust and sewage sludge in same operational conditions, respectively.

Figure 2b shows that the calculated curves are closely matched to the experimental curves by around 573 K for all mix ratios, above which slight differences are observed which can be explained within the levels of experimental repeatability. Moreover, the char yields at three heating rates are plotted against the blending ratios in Fig. 3. Strong linear distributions between the char yield and the blending ratios were established with an accuracy ≥ 0.995 . Physically, the release of volatile products during co-pyrolysis is expected to increase or decrease linearly in terms of the mass% pine sawdust share. Hence, it can be stated that there is no obvious occurrence of the synergistic activities during pyrolysis of sewage sludge and pine sawdust as a blend within the investigated experimental conditions, suggesting each component of the blends behaves as alone. However, Zhang et al. [24]. derived contradictory conclusions on the co-pyrolysis between sewage sludge and rice straw, which has obvious chemical interactions, not just a simple additive behavior. The different behaviors between sewage sludge and biomass during co-pyrolysis may be in part concerned with the uniqueness of the interlacing of biomass components for different classical biomass species [25]. There is a doubt that the release of volatile matter was accelerated in a very short time scale with the increase in the percentage of rice straw from 30 to 40 %, while the DTG curves of the two blends were nearly overlapped. Therefore, one other possible reason can be attributed to the inhomogeneity of the tested blends. However, it does not provide a ready explanation for the significant synergistic or coupling effects.

It is however worth noting that, even though the pine sawdust and sewage sludge pyrolysis rates have a broad temperature range where the main part of devolatilization overlaps, as pointed out in the previous section, this does not seem to allow non-additive behavior sufficiently. Considering the limited knowledge and studies about the synergistic effect between biomass and sewage sludge, one can conclude from some researches based on the thermal co-conversion of coal and biomass that synergy is highly dependent on the relative pyrolysis rates, the particle–volatiles, particle–particle, and volatiles–volatiles contact, and the matching of the release of individual fuel radical intermediates. For pyrolysis using a TG in nitrogen gas, the flow of nitrogen sweeps the volatile products, and prevents

them to remain close to the solid residue, which can shorten residence time and thus inhibit the secondary reactions. This shows that there is a lack of significant synergistic interactions between pine sawdust and sewage sludge in the solid phase under inert conditions, not including the gas–solid or gas–gas interactions. Therefore, further research should be required to fully shed light on the mechanism and conditions by which the two materials interact when mixed and transformed.

Effect of heating rates on pyrolysis characteristics

As the heating rate increases, the pyrolytic decomposition processes tend to delay in the direction of higher temperatures. The shape of these curves does not change markedly during this shift. This can mainly be attributed to the poor thermal conductivity exhibited by the studied samples, which signifies a temperature gradient existed throughout their cross section [26]. The temperature gradient within the particles increases along with the increasing heating rate. Under lower heating rate, if enough time can be given for heating, then both the exterior surface and the interior core of the fuels will attain same temperature at a specific time. On the contrary, the temperature profile along the cross section shows an appreciable difference to the higher heating rate, so this will result in serious thermal hysteresis.

The maximum degradation rate prominently increases when the heating rate is increased from 10 to 30 K min⁻¹, which can be assigned as being due to higher heat energy provided, thus facilitating better heat transfer between the surrounding environment and inside of the investigated materials [27]. These results are representative of the common trend of most non-isothermal experiments during the pyrolysis process. Regards to data shown in Table 2, however, there is no measurable effect of heating rate on the ending state of pyrolysis process for all of the samples. This result is in accordance with previous study for various biofuels [28, 29]. This is because the cross linking reactions may not be relevant under those investigated pyrolysis conditions, or there is equilibrium between the mechanism of cleavage bond breaking and repolymerization and cross linking, which lead to formation of gas products and char production, respectively [30].

Pyrolysis kinetics

Table 3 shows the change in apparent activation energy with progressing conversion degree for each sample calculated via the DAEM in detail. The correlation coefficients for the parameter estimation were also present. It is worth mentioning that at the end of the sewage sludge pyrolysis process, individual lines crossed each other,

Table 4 TG pyrolysis of apparent activation energies (E_A) and correlation coefficients for all samples at various conversion values using Friedman method and DAEM

Conversion = 50:50 %	Pine sawdust		PS/SS = 75:25 %		PS/SS		PS/SS = 25:75 %		Sewage sludge	
	$E_A/\text{kJ mol}^{-1}$	R^2	$E_A/\text{kJ mol}^{-1}$	R^2	$E_A/\text{kJ mol}^{-1}$	R^2	$E_A/\text{kJ mol}^{-1}$	R^2	$E_A/\text{kJ mol}^{-1}$	R^2
0.05	134.19	0.99	120.73	0.99	122.81	0.99	133.68	0.99	113.09	0.99
0.10	139.93	0.99	127.35	0.99	131.28	0.99	143.26	0.99	122.32	0.99
0.15	143.00	0.99	132.06	0.99	135.60	0.99	150.71	0.99	127.49	0.99
0.20	144.74	0.99	135.55	0.99	137.96	0.99	153.80	0.99	134.10	0.99
0.25	146.40	0.99	138.09	0.99	139.81	0.99	155.24	0.99	139.35	0.99
0.30	149.32	0.99	141.37	0.99	141.89	0.99	156.93	0.99	142.95	0.99
0.35	151.08	0.99	144.72	0.99	143.92	0.99	158.14	0.99	146.97	0.99
0.40	153.38	0.99	146.98	0.99	146.82	0.99	157.82	0.99	148.92	0.99
0.45	155.04	0.99	149.82	0.99	148.91	0.99	159.92	0.99	150.63	0.99
0.50	156.41	0.99	152.09	0.99	149.89	0.99	160.93	0.99	152.18	0.99
0.55	157.94	0.99	154.21	0.99	151.12	0.99	160.29	0.99	154.60	0.99
0.60	157.66	0.99	155.29	0.99	151.98	0.99	160.93	0.99	157.50	0.99
0.65	157.90	0.99	156.92	0.99	153.67	0.99	162.01	0.99	161.13	0.99
0.70	159.23	0.99	159.58	0.99	159.60	0.99	175.46	0.99	165.48	0.99
0.75	161.63	0.99	165.00	0.99	168.56	0.99	212.33	0.99	168.11	0.99
0.80	189.92	0.96	243.87	0.95	188.93	0.92	212.49	0.99	169.35	0.99
0.85	214.81	0.78	310.08	0.88	166.59	0.83	221.52	0.99	169.68	0.99
0.90	179.43	0.59	276.24	0.81	152.31	0.73	232.70	0.99	156.31	0.98
0.95	130.96	0.70	191.86	0.63	162.85	0.69	213.46	0.95	131.52	0.98

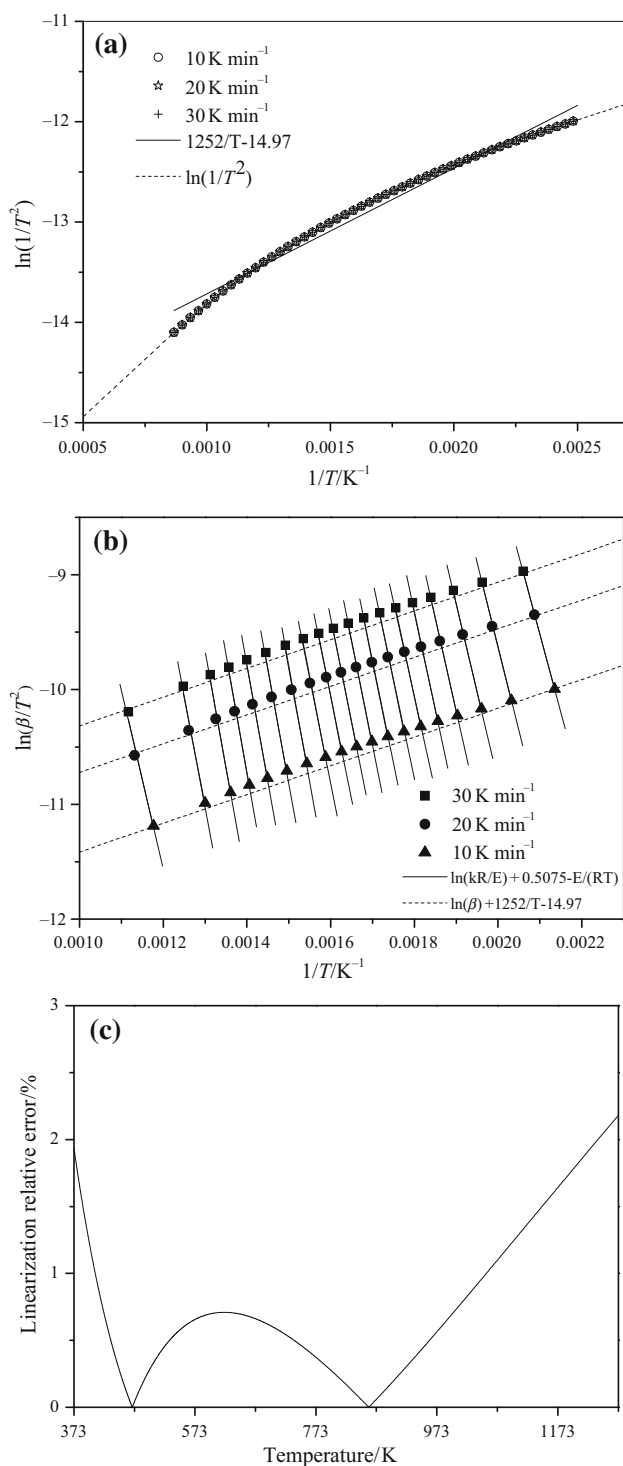


Fig. 5 **a** linearization of the $\ln(a/T^2)$ versus $1/T$ curves for various devolatilization rates, **b** linearization relative error, **c** determination of the temperature at which devolatilization of sewage sludge

resulting in a negative value of the apparent activation energy. So the final part of the decomposition lines should be cut off. For biomass and the blends with 75 and 50 mass% biomass fractions, since little correlation was

observed for the values of conversion above 0.8, the method worked for the range of conversion $0 \leq a \leq 0.8$. And with regard to sewage sludge and the blends with 75 mass% sludge fraction, because of the high correlation values it could account for the experimental curves in the complete range of conversion. This problem has been raised by the research of Fiori et al. [31], which was ascribed to the changed sequence of the temperature corresponding to same degrees of conversion at different heating rates over the entire conversion range.

Both differential isoconversional methods and integral methods have their own advantages and limitations [9]. The Miura–Maki DAEM as an advanced integral method provides a better option when backed up by the differential method of Friedman. The blend with 75 mass% sewage sludge fraction was selected as a representative of all samples for the presentation of the plots of the two methods, as can be seen clearly in Fig. 4, appearing no significant difference between the values of apparent activation energy calculated by Friedman method and DAEM. Similar results have been obtained for the others samples. Although the E_A determined by DAEM was smoother, the overall trends of E_A values obtained by Friedman method were broadly in line with that obtained by DAEM. Taking no account of the apparent activation energy corresponding to low correlation coefficient values, the average value of E_A calculated by Friedman method and DAEM are listed at Table 4. The results were in good agreement with a low deviation, which proves the validity of calculations of the DAEM.

The results of kinetic analysis showed that apparent activation energy varies significantly with conversions for all species studied, which indicates a high probability existed for the presence of multi-step mechanism. In case of all studied samples, the same overall trend was observed: the apparent activation energy increased gradually to reach a maximum value in the conversion range, 0.05–0.8. This result of pine sawdust is in agreement with some reports based on several similar types of biomass [32] but in contrast with a few others [33]. Therefore, for complex materials, the theoretical interpretation of the apparent activation energy trend may be unreliable. The activation energy determined by the isoconversional methods can be used in applications without interpretation but for obtaining mechanistic clues [9]. Actually, the physical meaning of apparent activation energy remains somewhat ill-defined, thus no conclusions could be drawn. The emphasis is to estimate the modeled physical quantities [34]. The conversion rate of pine sawdust was 0.05–0.8 at apparent activation energy of 134–190 kJ mol⁻¹, which was consistent with previous reports [35]. The activation energy of sewage sludge ranged from 113 to 170 kJ mol⁻¹ within the conversion rate of 0.05–0.95. Because of the

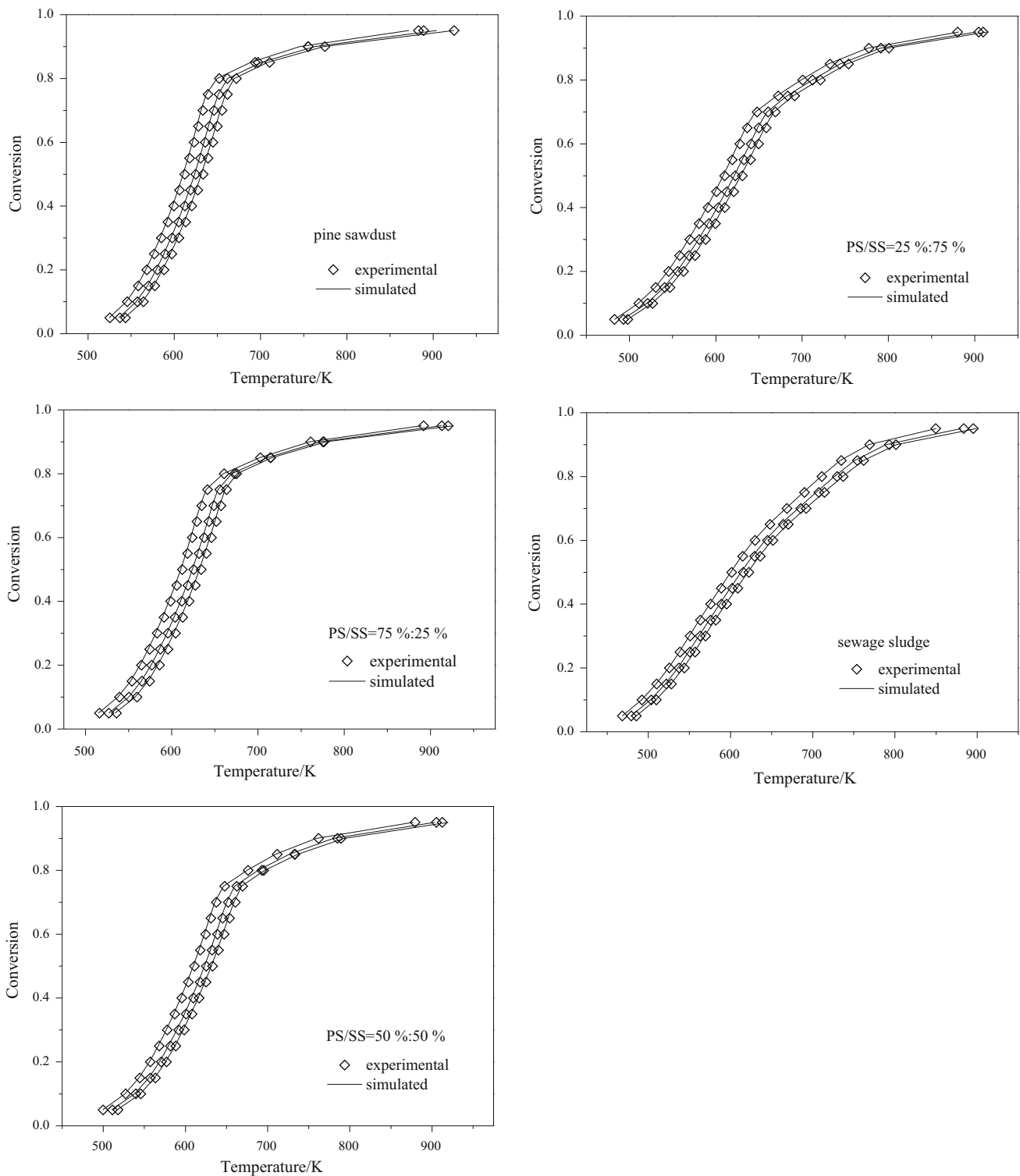


Fig. 6 Comparisons of experimental and simulated conversion curves (experimental curves depicted by *shaped markers* and predicted curves depicted by *lines*)

considerably variable characteristics of different sewage sludge, it is difficult and ambiguous to make a direct comparison on the results obtained in the pyrolysis between our sewage sludge sample and the others. For the

three blends studied, the activation energy range was from 121 to 244 kJ mol^{-1} . When comparing with the pure materials, the apparent activation energy of sewage sludge does not change significantly in the presence of biomass,

and the effect of adding sewage sludge with biomass was also very slight.

To validate the predictive power of Miura–Maki DAEM, a simplified method proposed was used. The $\ln(1/T^2)$ versus $1/T$ for the data points used are shown in Fig. 5a, combined with the linearization. One can observe that the three curves collapsed due to the disappearance of heating rates. Obviously, these data points form a conical section in the plot; nevertheless, the linearization relative error between the linearization and the conical section is really small within the usual temperature range of 413–1,093 K, as shown in Fig. 5b. In Fig. 5c, the temperature for a determined devolatilization rate can be obtained from the intersection between the linearization for each devolatilization rate and the linearization for a heating rate. Hence, using the two equations shown in the plot, the temperature at which devolatilization occurs can be calculated in the following equation:

$$T = \frac{-E_A/R - 1252}{\ln(\beta) - \ln\left(\frac{kR}{E_A}\right) - 15.58} \quad (8)$$

Utilizing Eq. (8), Fig. 6 reports the experimental data for each sample at three heating rates along with the model curves regarding the simplified method. It seems the fitting satisfies for all cases. The accuracy of simulation can be evaluated by the relative error R between the experimental data and the simplified method output:

$$R = \frac{|T_{\text{exp}} - T_{\text{est}}|}{T_{\text{exp}}} \times 100 \%, \quad (9)$$

where T_{exp} represents the experimental temperature at which each devolatilization occurs, T_{est} represents the corresponding estimated temperature calculated by the simplified method. The maximum relative error is less than 0.35 and 0.31 % for sewage sludge and the blend with 75 mass% sewage sludge, respectively, enabling utilization of the model throughout the whole range of conversions. However, the fitting was less perfect in the high temperature range for the biomass and the blends with 75 and 50 mass% biomass fractions, since the relative error was up to a value of 1.59 %. Apart from these high temperature range, a good match can be obtained within the restricted range of conversion $0 \leq a \leq 0.8$, as the relative error is no more than 0.49 %. A tendency can be found for all tested blend samples, obtaining better predicted performance with the increased percentage of sewage sludge. In general, the simulation for all studied samples can be considered accurate.

Conclusions

The thermal behavior and thermokinetics of the co-pyrolysis of sewage sludge and pine sawdust were investigated

via non-isothermal thermogravimetric analysis. Characterization of pine sawdust and sewage sludge demonstrated that PS contained the highest amount of calcium, and SS had a high percentage of ash. TG mass loss data showed that there existed three stages during the pyrolysis of PS and SS. The weighted average of DTG data of PS and SS agreed closely with that of the blends, and a perfect linear relationship was shown between final char yield and fraction of sludge in the blends. Therefore, it may be concluded that the interactions between the two materials in the blends are slight under the conditions used in the study. The average values of apparent activation energy for the three blends calculated by Friedman method and DAEM were 152.39–175.39 and 148.05–172.72 kJ mol⁻¹, respectively. The DAEM model served as a good method to describe the devolatilization process of the blends, since good match were observed between the experimental and the calculated conversion (a - T) curves.

Acknowledgements The work described in this paper was financially supported by SRF for ROCS, SEM, China, Fundamental Research Funds for the Central Universities (2013TS070, Cxy13q030.cx14-011.cx14-012.01-09-070098), the National Natural Science Foundation of China (21276100), and Hubei Provincial Natural Science Foundation, China (No. 2014CFB441). The authors are also grateful to Cai Junmeng (Shanghai Jiao Tong University) who provided valuable comments and suggestions to the pyrolysis kinetic analysis.

References

- Manara P, Zabaniotou A. Towards sewage sludge based biofuels via thermochemical conversion—a review. *Renew Sust Energy Rev.* 2012;16:2566–82.
- Werle S, Wilk RK. A review of methods for the thermal utilization of sewage sludge: the Polish perspective. *Renew Energy.* 2010;35:1914–9.
- Di Blasi C. Modeling chemical and physical processes of wood and biomass pyrolysis. *Prog Energ Combust.* 2008;34:47–90.
- Rulkens W. Sewage sludge as a biomass resource for the production of energy: overview and assessment of the various options. *Energy Fuel.* 2007;22:9–15.
- Pinto F, André RN, Lopes H, Dias M, Gulyurtlu I, Cabrita I. Effect of experimental conditions on gas quality and solids produced by sewage sludge cogasification. 2. Sewage sludge mixed with biomass. *Energy Fuel.* 2008;22:2314–25.
- Várhegyi G. Aims and methods in non-isothermal reaction kinetics. *J Anal Appl Pyrolysis.* 2007;79:278–88.
- Vyazovkin S. Two types of uncertainty in the values of activation energy. *J Therm Anal Calorim.* 2001;64:829–35.
- Burnham AK, Dinh L. A comparison of isoconversional and model-fitting approaches to kinetic parameter estimation and application predictions. *J Therm Anal Calorim.* 2007;89:479–90.
- Vyazovkin S, Burnham AK, Criado JM, Pérez-Maqueda LA, Popescu C, Sbirrazzuoli N. ICTAC kinetics committee recommendations for performing kinetic computations on thermal analysis data. *Thermochim Acta.* 2011;520:1–19.
- Várhegyi G, Szabó P, Antal MJ. Kinetics of charcoal devolatilization. *Energy Fuel.* 2002;16:724–31.

11. Zhao HY, Cao Y, Sit SP, Lineberry Q, Pan WP. Thermal characteristics of bitumen pyrolysis. *J Therm Anal Calorim.* 2012;107:541–7.
12. Li C, Suzuki K. Kinetic analyses of biomass tar pyrolysis using the distributed activation energy model by TG/DTA technique. *J Therm Anal Calorim.* 2009;98:261–6.
13. Li L, Wang G, Wang S, Qin S. Thermogravimetric and kinetic analysis of energy crop Jerusalem artichoke using the distributed activation energy model. *J Therm Anal Calorim.* 2013;114:1183–9.
14. Herce C, de Caprariis B, Stendardo S, Verdone N, De Filippis P. Comparison of global models of sub-bituminous coal devolatilization by means of thermogravimetric analysis. *J Therm Calorim.* 2014;117:507–16.
15. Please C, McGuinness M, McElwain D. Approximations to the distributed activation energy model for the pyrolysis of coal. *Combust Flame.* 2003;133:107–17.
16. Cai J, Ji L. Pattern search method for determination of DAEM kinetic parameters from nonisothermal TGA data of biomass. *J Math Chem.* 2007;42:547–53.
17. Miura K, Maki T. A simple method for estimating $f(E)$ and $k_0(E)$ in the distributed activation energy model. *Energy Fuel.* 1998;12:864–9.
18. Soria-Verdugo A, Garcia-Hernando N, Garcia-Gutierrez L, Ruiz-Rivas U. Analysis of biomass and sewage sludge devolatilization using the distributed activation energy model. *Energy Convers Manag.* 2013;65:239–44.
19. Yang H, Yan R, Chen H, Lee DH, Zheng C. Characteristics of hemicellulose, cellulose and lignin pyrolysis. *Fuel.* 2007;86:1781–8.
20. Whitely N, Ozao R, Cao Y, Pan W-P. Multi-utilization of chicken litter as a biomass source. Part II. Pyrolysis. *Energy Fuel.* 2006;20:2666–71.
21. Biagini E, Lippi F, Petarca L, Tognotti L. Devolatilization rate of biomasses and coal–biomass blends: an experimental investigation. *Fuel.* 2002;81:1041–50.
22. Francioso O, Rodriguez-Estrada MT, Montecchio D, Salomoni C, Caputo A, Palenzona D. Chemical characterization of municipal wastewater sludges produced by two-phase anaerobic digestion for biogas production. *J Hazard Mater.* 2010;175:740–6.
23. Ghetti P, Ricca L, Angelini L. Thermal analysis of biomass and corresponding pyrolysis products. *Fuel.* 1996;75:565–73.
24. Shuang-quan Z, Xiao-ming Y, Zhi-yuan Y, Ting-ting P, Ming-jian D, Tian-yu S. Study of the co-pyrolysis behavior of sewage-sludge/rice-straw and the kinetics. *Procedia Earth Planet Sci.* 2009;1:661–6.
25. Morgan TJ, Kandiyoti R. Pyrolysis of coals and biomass: analysis of thermal breakdown and its products. *Chem Rev.* 2013;114:1547–607.
26. Maiti S, Purakayastha S, Ghosh B. Thermal characterization of mustard straw and stalk in nitrogen at different heating rates. *Fuel.* 2007;86:1513–8.
27. Caballero J, Front R, Marcilla A, Conesa J. Characterization of sewage sludges by primary and secondary pyrolysis. *J Anal Appl Pyrolysis.* 1997;40:433–50.
28. Jeguirim M, Trouvé G. Pyrolysis characteristics and kinetics of *Arundo donax* using thermogravimetric analysis. *Bioresour Technol.* 2009;100:4026–31.
29. Luangkiattikhun P, Tangsathitkulchai C, Tangsathitkulchai M. Non-isothermal thermogravimetric analysis of oil-palm solid wastes. *Bioresour Technol.* 2008;99:986–97.
30. Di Nola G, De Jong W, Spliethoff H. TG-FTIR characterization of coal and biomass single fuels and blends under slow heating rate conditions: partitioning of the fuel-bound nitrogen. *Fuel Process Technol.* 2010;91:103–15.
31. Fiori L, Valbusa M, Lorenzi D, Fambri L. Modeling of the devolatilization kinetics during pyrolysis of grape residues. *Bioresour Technol.* 2012;103:389–97.
32. Biagini E, Fantei A, Tognotti L. Effect of the heating rate on the devolatilization of biomass residues. *Thermochim Acta.* 2008;472:55–63.
33. Aboyade AO, Hugo TJ, Carrier M, Meyer EL, Stahl R, Knoetze JH, et al. Non-isothermal kinetic analysis of the devolatilization of corn cobs and sugar cane bagasse in an inert atmosphere. *Thermochim Acta.* 2011;517:81–9.
34. Šimon P, Thomas P, Dubaj T, Cibulková Z, Peller A, Veverka M. The mathematical incorrectness of the integral isoconversional methods in case of variable activation energy and the consequences. *J Therm Anal Calorim.* 2014;115:853–9.
35. Sichone K. Pyrolysis of sawdust. PhD thesis. University of Waikato. 2013.